Séminaire Poincaré XII (2009) 45 – 73 Séminaire Poincaré

Studies of DNA-Replication at the Single Molecule Level Using Magnetic Tweezers

M. Manosas, T. Lionnet, E. Praly, D. Fangyuan,
J.-F. Allemand, D. Bensimon, and Vincent Croquette
LPS, ENS
UMR 8550 CNRS
24, rue Lhomond
75231 Paris Cedex 05, France

Abstract. The development of tools to manipulate single biomolecules has opened a new vista on the study of many cellular processes. In this review we will focus on the use of magnetic tweezers to study the behavior of enzymes involved in DNA replication. Depending on the DNA substrate used, magnetic tweezers give access either to the advancement in real time of the so-called replication fork or to the torsional state (the so-called supercoiled density) of the DNA molecule. We will show how the new tools at our disposal can be used to gain an unprecedented description of the kinetic properties of enzymes. The comparison of these results with theoretical models allows us to get insight into the mechanism used by the enzymes under study. This analysis is often out of reach of more classical, bulk techniques.

1 Introduction

Biophysics is currently undergoing an important transformation due to the development of tools for manipulating, visualizing and studying single molecules and their interactions. New tools such as optical or magnetic tweezers, have allowed the manipulation of single DNA molecules and a detailed characterization of their elastic response (see [1] for review). These experiments have renewed theoretical interest in the mechanical properties of biomolecules. Consequently, we presently have a very good understanding of the response to tension and torsion of DNA over a large range of forces and torques [2]. Modification of these elastic properties induced by proteins that bind to DNA provides precious information about DNA-protein interactions and enzymatic kinetics. Proteins that alter the DNA's extension or the DNA's topological conformation can be studied at the single molecule level by using these tools. Moreover, whenever the time resolution of the measuring device is sufficient, these studies permit real time monitoring of the DNA/protein interaction.

These micromanipulation experiments introduce force as a new thermodynamic parameter in *in vitro* experiments. Force can be used to alter the equilibrium of a reaction or modify its activation barriers, in addition to the temperature or buffer conditions, which are often the only control parameters in a conventional bulk assays [3, 4, 5]. Moreover, these single-molecule investigations avoid the ensemble averaging inherent in bulk measurements. Such averaging may hinder the observation of some dynamical properties of the enzyme or obscure the existence of an heterogeneous

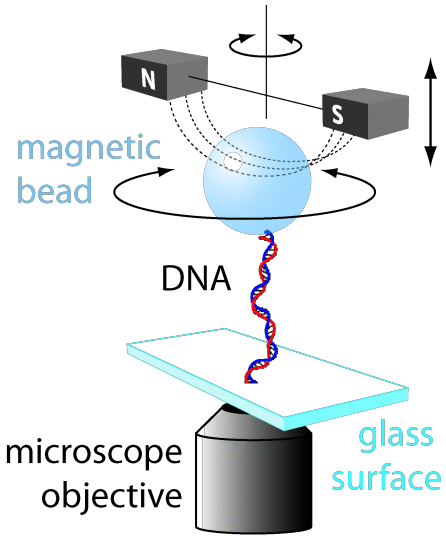

Figure 1: Magnetic tweezers set-up. A DNA molecule is anchored at one end to a micron sized magnetic bead and at the other to the bottom surface of a square capillary tube, placed on top of a microscope objective. Small magnets placed above the sample can be used to pull and twist the DNA molecule.

population. Single molecule assays only measure active enzymatic complexes, in contrast to conventional biochemical experiment where the intrinsic enzymatic activity is estimated by dividing the total activity by the concentration of enzymes, an estimate that often underestimates the real activity if a large portion of the enzymes are inactive or if the active complex is multimeric.

In the present review, after a short introduction to magnetic tweezers and a summary of the elastic properties of bare DNA molecules, we will present some of the results obtained in our group concerning the study of the DNA replication.

2 Magnetic tweezers

Most of the enzymes involved in DNA replication are molecular motors which convert the energy from NTP (or dNTP) hydrolysis into mechanical work. The hydrolysis of a single molecule of ATP, under physiological conditions, generates about 20 k_BT (i.e. $8 \cdot 10^{-20} J$) of energy (k_B is Boltzmann constant and $T \sim 300$°K room temperature). Since the characteristic displacement of a biological motor is on the order of a few nanometers, the relevant forces for micromanipulation of biological molecules are on the order of: $8 \cdot 10^{-20} J / 10^{-8} m \sim 8 \cdot 10^{-12}$ N. To apply and detect such forces different techniques have been developed: Atomic Force Microscopy [6], Biomembrane Force Probe [7], glass micropipette manipulation [8], flow induced force [9], optical [10] and magnetic tweezers (see [2] and references therein). For the purpose of this review, we provide only a brief description of magnetic tweezers.

Magnetic tweezers are used to manipulate magnetic beads tethered to a surface by a DNA molecule (but potentially by any polymer). When placed in the magnetic field of permanent (or electro-) magnets (see Fig.1), their magnetic dipole experiences both a force F (parallel to the magnetic field gradient) and a torque Γ (that tends to align its dipole with the magnetic field). A micron size bead at a distance

of one millimeter of a pair of two NdFeB magnets separated by a half millimeter gap, is pulled by a force of a few pN towards the high magnetic field region. By varying the distance between the bead and the magnets we modulate the force between 20 pN to a few femtonewtons. Interestingly, such force values fall in the range of biological forces. On the other hand, the torque applied to the bead can reach 10^5pN.nm, a value that exceeds any biological torque. Thus the bead magnetization follows closely that of the magnetic field.

Since beads are not perfectly uniform in size and magnetization and the force is a very nonlinear function of the distance between the bead and the magnets, the exact value of the force applied by this tweezers must be calibrated. The latter is achieved by measuring the Brownian fluctuations. The beads are subject to Brownian fluctuations and exhibit random displacements transverse to the direction of the pulling force. The amplitude of such fluctuations is inversely proportional to F: the stronger the force the less the bead fluctuates. In fact, the bead tethered by a DNA molecule of extension l and pulled by the magnetic field is similar to a damped pendulum. Applying the dissipation-fluctuation theorem to this system, yields a relation between the force and the amplitude of the transverse fluctuations $< \delta x^2 >$: $F = k_B T l / < \delta x^2 >$. Video microscopy allows measurement of the three dimensional position of the bead with nanometer resolution [11] and thus of l and $< \delta x^2 >$. Using this Brownian motion method, forces from a few femtoNewtons to a hundred of picoNewtons have been measured [11]. The magnetization of the bead presents no hysteresis. Therefore once the force versus magnet distance has been determined for several beads (see Fig. 2), we can use the average measured relation to predict the force according to the magnet distance. It turns out that the bead magnetization distribution is pretty narrow and the force acting on a bead may be predicted without previous calibration with a typically error of 20% (see Fig. 2). This accuracy is sufficient for many experiments.

A distinct advantage of magnetic tweezers is that they are intrinsic force clamps: the force applied to the bead is controlled and the extension of the molecule is measured. Other micromanipulation systems (e.g. optical tweezers) are natural extension clamps, distances are imposed and the force is measured. In those systems the application of a constant force requires implementation of a feedback loop [12]. In addition, rotating the bead to impose a torque on the molecule is extremely simple using magnetic tweezers, thus permitting control over the topological state of the DNA under study.

2.1 Finding beads tethered by a single molecule

To prepare a single molecule assay, one usually mixes streptavidin coated beads with modified DNA molecules having biotin at one end and digoxigenin at the other end. The DNA molecule will diffuse until its biotinylated end links to the streptavidin coated bead. By flowing gently these beads in a microchannel coated with antidigoxigenin, the DNA molecule may tether a bead to the micro-channel glass plate. To work in the single molecule limit, we use a small number of DNA molecules compared with that of the magnetic beads. In general, this protocol works very efficiently. Nevertheless, the probability of having one bead tethered to the glass substrate by two or more DNA molecules is not zero. Therefore, when we select a bead for further study our first task is to insure that it is indeed tether by a single molecule.

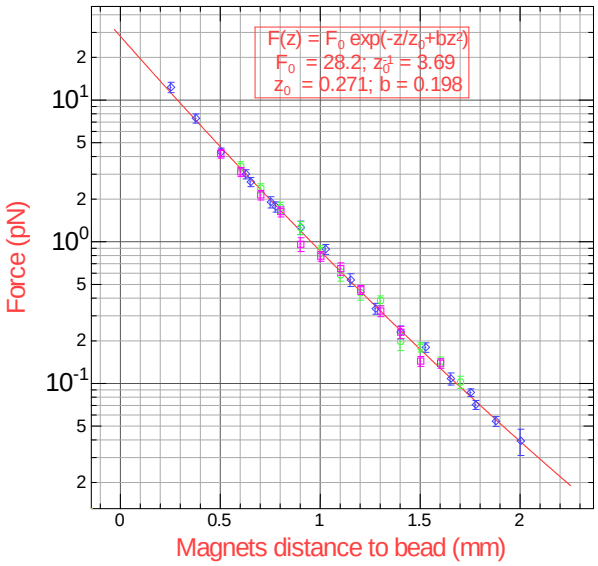

Figure 2: Force measured on a micron-sized bead versus the distance from the magnets. This calibration is done using the Brownian motion method. The curve may be fitted by a simple formula (full red line). Three different beads are compared on this graph (blue, magenta and green points). The force agrees for these three beads within the experimental error.

Rotating the magnets offers a very convenient mean to answer this critical question. The assay will depend on the exact molecule used. If we are dealing with single stranded DNA or nicked double stranded DNA, the molecule will be completely insensitive to torsion. In this latter case, if the bead is tethered by a single molecule its position (specially its vertical one) remains unchanged when we rotate the magnets by a significant number of turns. On the contrary, if it is tethered by two or more molecules, the bead rotation entangles the molecules inducing a reduction of the molecule extension. This test is quick and extremely simple. If we use a dsDNA molecule specially prepared to sustain torsion, the test is a little more complex since this time the molecule extension is sensitive to torsion. However, the occurrence of phase transitions such as DNA denaturation or PDNA [13] offers a mean to identify a possible single molecule tether. In any case, measuring the force extension curve of the tether is an ultimate single molecule test.

3 How stretching and twisting DNA helps to track replication process

3.1 Stretching a polymer model: dsDNA

The double stranded DNA (dsDNA) molecule is a long, double helical polymer. This particular secondary structure confers interesting mechanical properties to the molecule. Understanding such properties is crucial before studying the behavior of DNA bound motors as their action might induce changes in the DNA's extension and topology. Furthermore their activity might be controlled by the torque or the force on the molecule.

Like any polymer in solution, dsDNA adopts a random coil geometry that maximizes the number of accessible conformations and thus the entropy. As one starts

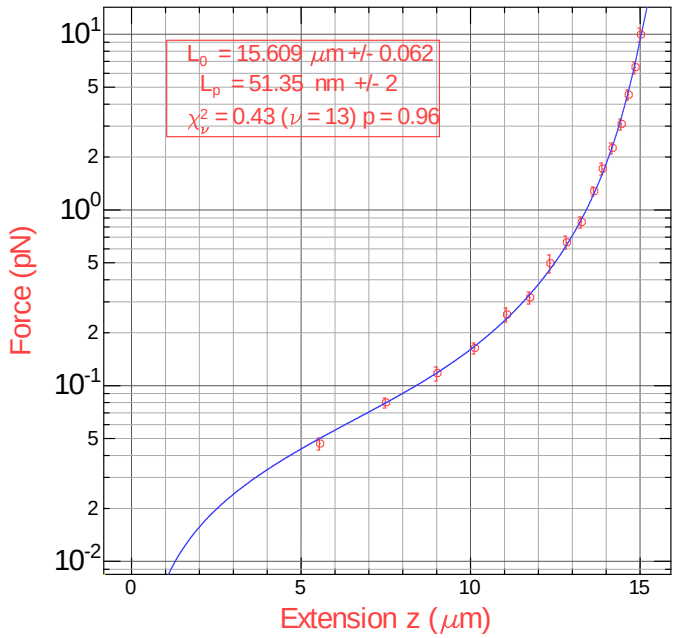

Figure 3: Force extension curves of a dsDNA molecule.[14].

to stretch dsDNA, the molecule tends to align along the force axis, which decreases the number of accessible conformations. Such decrease in entropy dictates the magnitude of the stretching force. This so-called entropic regime of forces lasts until the molecule is fully aligned (with a single conformation allowed) at a force $F \sim 10$pN. In that regime the elastic response of dsDNA is well described as a flexible tube with bending rigidity B (Worm-Like Chain (WLC) model). At any given force, the extension of the molecule l is determined by minimizing its free energy (*i.e.* weighting the loss in bending energy against the gain in entropy [15],[16]).

The fit of the experimental force-extension data yields a persistence length (*i.e.* the typical length over which thermal fluctuations can bend the DNA) $\xi = B/k_BT = 52$ nm [16] under physiological conditions, see Fig.3. This value is high compared to common man-made polymers (with $\xi \sim 1-2$ nm) because the base stacking at the molecule's core stiffens it. Using this value of ξ, we can estimate the mean radius R_0 of the *E. coli* chromosome: $R_0 = \sqrt{2L\xi} \simeq 10$ μm, (L being the length of the DNA, $\simeq 1$ mm). The comparison of this value to the typical *E. coli* size of 1 μm suggests that the cell must have more efficient ways to compact its DNA. This is indeed achieved by specific DNA-compacting proteins (e.g. condensins) and by supercoiling the molecule.

3.2 Twisting dsDNA

The behavior of DNA under torsion can be explored with magnetic tweezers by simply rotating the magnets and thereby the bead tethered by a dsDNA. At low twist, the DNA's extension is not affected significantly by the torsion. However when the number of turns imposed on the molecule is large enough it buckles under the torsional load. Additional turns applied to the molecule make it writhe and form plectonemic loops, Fig.4. Thus its extension decreases linearly with the applied

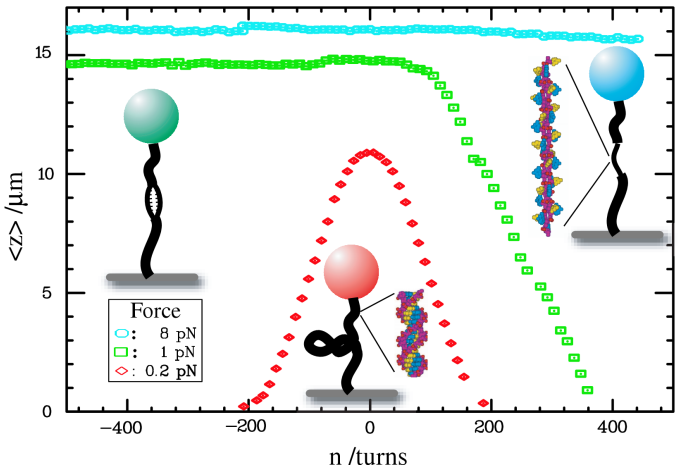

Figure 4: DNA twisting at various forces. At low forces (red), as the molecule is over or underwound its extension decreases identically by forming left or right-handed plectonemes. At intermediary forces (green), negatively supercoiled DNA denatures, while left-handed plectonemes can still be observed for positive supercoiling. At high forces (blue), positively supercoiled DNA undergoes a transition to an inside-out structure called P-DNA [13].

number of turns, n. The partitioning of the excess linking number ΔLk (a topological constant here equal to n) between writhe (plectonemes) and twist (change of the helical pitch) plays a key role in major cellular processes, such as DNA compaction, replication or transcription. The formation of plectonemes is observed symmetrically under positive and negative torsion, as long as the stretching force is held below a (salt dependent) critical force, typically $F \sim 0.5$ pN. However above this force, the critical torque for denaturation is smaller than the critical torque for buckling Γ_c (which increases as $\Gamma_c \sim F^{1/2}$). In this case, a negatively supercoiled DNA will respond to a large unwinding by denaturing rather than by forming plectonemic loops [17].

3.3 Stretching ssDNA

The elastic behavior of ssDNA, unlike that of dsDNA, strongly depends on the salt conditions and the chain's nucleotide content. It cannot be fitted by a simple elastic polymer model such as the WLC model. First ssDNA is much more flexible than ds-DNA: its persistence length ($\xi_{ssDNA} \sim 1.6$ nm) is about 30 times smaller. Therefore, the electrostatic repulsion between the charged phosphates on its backbone cannot be neglected (as they are for dsDNA), since they are screened over a Debye length that is similar to ξ_{ssDNA}. Second, ssDNA is a somewhat peculiar polymer: because of the possibility of pairing between the bases along its backbone, it is able to form hairpin structures at low forces, which are highly sequence- and salt-dependent. All these effects can be incorporated (with some approximations) in a Monte Carlo (MC) simulation of a chain under tension. These simulations turn out to nicely describe the behavior of ssDNA over a large range of forces and ionic strengths [14]. Even though a complete theoretical understanding of the elastic behavior of ssDNA is still lacking, the experimental evidence clearly shows that (except near $F \sim 5$ pN) ssDNA and dsDNA have different extensions. As we shall see below this difference

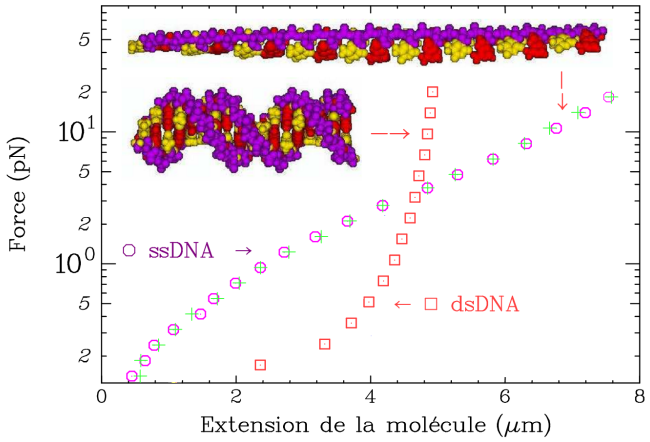

Figure 5: Force extension curves of single stranded (green and magenta points) and double stranded (blue points) DNA. The dsDNA data was fitted to a WLC model (blue line) with persistence length $\xi = 52$ nm. The ssDNA data show that the molecule is shorter than dsDNA when force is smaller than 5pN and longer above.[14].

can be used to monitor the action of enzymes such as helicases or DNA-polymerases that transform dsDNA into ssDNA or vice-versa.

3.4 Unzipping DNA

Many DNA substrates may be studied using magnetic tweezers. Let us discuss one which will be of interest when studying the replication fork. It consists of a single stranded DNA molecule having a partial palindromic sequence in its center. This palindromic part of the molecule spontaneously folds forming a double stranded DNA molecule closed at one end by a short loop while the two non-complementary parts form a fork (see Fig. 6A). Using biochemistry, we modify the two ends of the DNA molecule attaching biotin at one extremity and digoxigenin at the other. Beads incubated with such DNA molecules are next inserted into the magnetic tweezers chamber. To test whether a magnetic bead has a DNA molecule attached we increase the stretching force until 15 pN, force required to unzip the molecule (see Fig. 6 B). At that force the hydrogen bonds between base pairs are broken and the extension of the molecule abruptly increases. Each time a base pair opens, the extension increases by approximately 1 nm, as expected from single strand DNA elasticity.

When the molecule is fully open, it may refold if the force is lowered. However, this process is controlled by a critical step involving the refolding of the loop in the middle of the palindromic sequence. This loop formation requires a fluctuation having a significant energy to bring in contact base pairs which are separated. The time needed to overcome this critical step diverges as the force increase close to the unzipping force. Thus there is a substantial hysteresis in the molecule refolding as shown in Fig. 6.

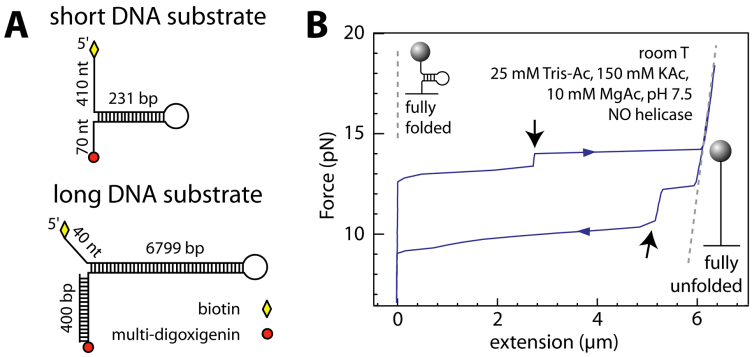

Figure 6: (A) Single stranded DNA molecules having a palindromic sequence. This sequence leads to the formation of a hairpin structure: the molecule refolds and presents a dsDNA structure. The biotin molecule binds this molecule on the streptavidin coated bead, while the digoxigenin at the other end of the molecule links to the glass substrate. When a force is applied it pulls apart the hairpin in an unzipping action. Two DNA substrates have been studied which differ in their lengths (231 bp and 6799 bp) and GC contents (32% and 42 % respectively). (B) Typical force vs. extension curve observed for the long DNA hairpin. As the force is increased to 14 pN, the molecule abruptly extends, and finally reaches its full length $6\ \mu m$. Refolding of the DNA molecule occurs at a lower force (F $\approx$ 11 pN). Unfolding and refolding transitions display intermediates (arrows), which corresponds to metastable positions of the fork along the hairpin sequence.

4 Study of the Replisome

In the cell, DNA replication is carried out by a multiprotein complex known as the replisome. Replisomes from different organisms vary in size and complexity. For example, only four proteins are needed to assembly the bacteriophage T7 replisome [18], whereas tens of proteins are required in eukaryotes [19]. Despite the differences in the number of proteins involved, many components of the replisome are functionally and structurally conserved from organism to organism. Studies in prokaryotic and viral systems have contributed greatly to our present understanding of DNA replication [20].

One of the model systems used to study DNA replication is the bacteriophage T4 replisome. The bacteriophage T4 presents a simple yet interesting replisome having eight proteins, a number small enough to be handled and sufficiently large compared with the seven different activities of the replisome. These eight proteins together have been shown to reconstitute in vitro leading and lagging strand DNA synthesis [20].

4.1 The T4 replisome components

The leading and lagging strand templates are copied by two holoenzyme complexes, each composed of the polymerase (gp43) and the clamp (gp45) [21]. The clamp protein is loaded by the clamp loader complex (gp44/62) in an ATP-dependent fashion [22, 23]. DNA polymerases can only synthesize nascent DNA in the 5' to 3' direction; therefore, the leading strand holoenzyme may copy the DNA template continuously, while the lagging strand holoenzyme must copy the DNA template in the opposite direction from the fork movement. This process can only be done

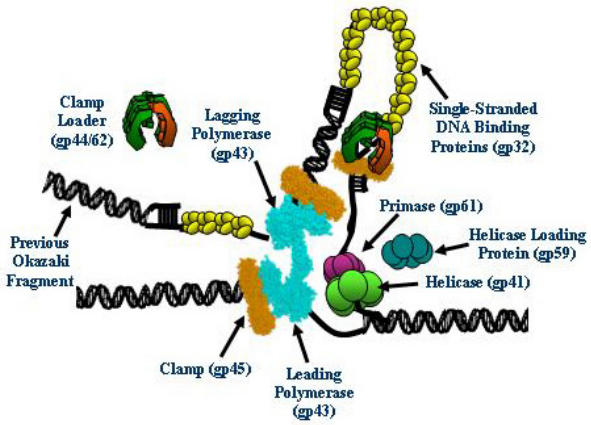

Figure 7: Sketch of the replisome around a DNA replication fork. The gp41 helicase opens the DNA and gp61 is the primase that synthesizes a small RNA primer required for initiation of Okazaki fragment synthesis. On both strands, the DNA is copied by the gp43 polymerase which stability is enhanced by the gp45 clamp. The helicase, the primase and the polymerase have each a special protein complex which helps their loading on the DNA substrate. The single stranded binding protein gp32 covers the single stranded DNA molecule that appears transiently in this process.

sequentially in short segments known as Okazaki fragments approximately 1 kb in size. The primosome is a subassembly acting in front of the replisome composed of a hexameric helicase (gp41) that unwinds dsDNA by translocating along the lagging strand template in the 5' to 3' direction [24] and an oligomeric primase (gp61) that synthesizes pentaribonucleotide primers at 5-GTT and 5-GCT sequences to initiate repetitive Okazaki fragment synthesis [25, 26]. In the presence of single-stranded DNA binding protein (gp32), which coats the ssDNA produced by the helicase [27], the primosome requires a helicase accessory protein (gp59) for efficient loading [28, 29].

The work presented here focuses on the study of the enzymes of the T4 replisome, and the interactions between them. In particular, we have investigated two sub-assemblies of the replisome: the primosome and the holoenzyme. The primosome is the assembly of the helicase and the primase and it is responsible for unwinding the DNA and initiation of Okazaki fragments. The holoenzyme which copies the DNA is the complex formed by the polymerase and the clamp and it requires the clamp loader to be efficiently loaded. Leading strand synthesis is achieved by combining holoenzyme and helicase activities.

4.2 A simple replication fork

The replisome as presented on Fig. 7 is a fascinating but complex molecular object. Observing the activity of all its components at once at the single molecule might be hard and results difficult to interpret. Our strategy consist of first studying individual proteins. Once the behaviour of each component is well characterized, we can start studying protein sub-assemblies within the replisome to get insight into its functioning. Finally by progressively increasing the number of proteins we aim to build up the full replisome.

We have prepared a simplified version of the replication fork which consists of

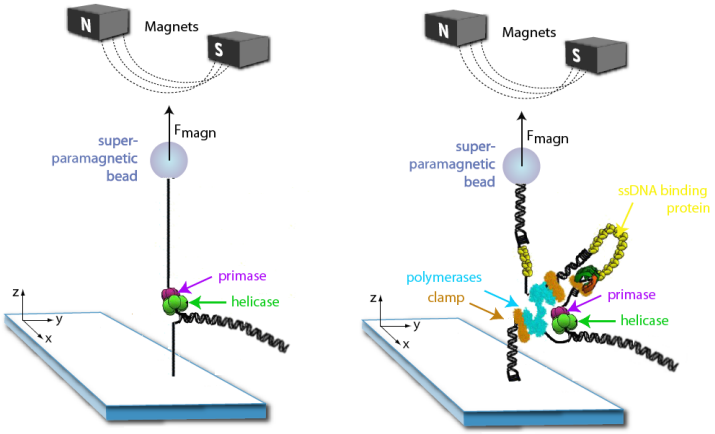

Figure 8: Sketch of different steps in the replisome study. On the left, a simple DNA fork is unwound by the helicase alone or associated with the primase. On the right, the full replisome unwinds and duplicates the two strands of the DNA hairpin. In both cases, the extension of the molecule is used to follow in real time the motion of the enzymes. The force applied on the bead is kept below 11 pN ensuring that the changes in DNA extension are the result of enzymatic activity of proteins on the DNA and not mechanical manipulation.

a single stranded DNA molecule forming a hairpin (the DNA molecule used in the unzipping assay presented previously). Experiments were carried out by tethering a DNA hairpin between a glass surface and a magnetic bead (Fig. 8) Different DNA substrates were used with variable duplex lengths (from 231 bp up to 6.8 kbps). We use these templates in our magnetic tweezers setup. Using one micron bead, the force may reach 20 pN.

4.3 Helicase, polymerase and replisome assays

The basis of the assay is the following: either the activity of isolated proteins such as gp41 helicase and gp43 polymerase or the activity of the full replisome will induce the unwinding of the hairpin. Thus their activity can be detected as an increase in the end-to-end distance of the DNA molecule observed as a change in the distance between the bead and the surface (Fig. 8).

We initially characterize the mechanical unfolding of the hairpin construct in the absence of proteins. Mechanical unfolding resulting in an extension of the DNA molecule occurs at a typical range force of 14-17 pN depending on the substrate and displays a marked hysteresis as seen on Fig. 6. Typically at forces of 12 ± 1pN the hairpin is stably folded for the duration of a typical experiment. Therefore below 12 ± 1 pN of force, any unfolding observed in the presence of proteins results from their activity. Indeed in absence of any helicase and polymerase, the extension of the DNA molecule remains constant at the level corresponding to the folded hairpin.

After this calibration, the DNA hairpin is held at a constant force below the unfolding transition force and a buffer containing the proteins under study is injected into the experimental chamber while the extension of the molecule is recorded over time. Any change in extension is thus due to an interaction of the proteins with the DNA (unwinding, polymerization, DNA looping, dissociation, or translocation on ssDNA).

5 Characterizing the helicase activity

The gp41 helicase is active as an hexameric ring [30] that encircles ssDNA and unwinds the DNA with 5' to 3' polarity [31]. Within the full replisome is able to promote DNA unwinding at rates of 300-400bp/s [32, 33]. Here we have studied its unwinding and translocation activity at the single molecule level.

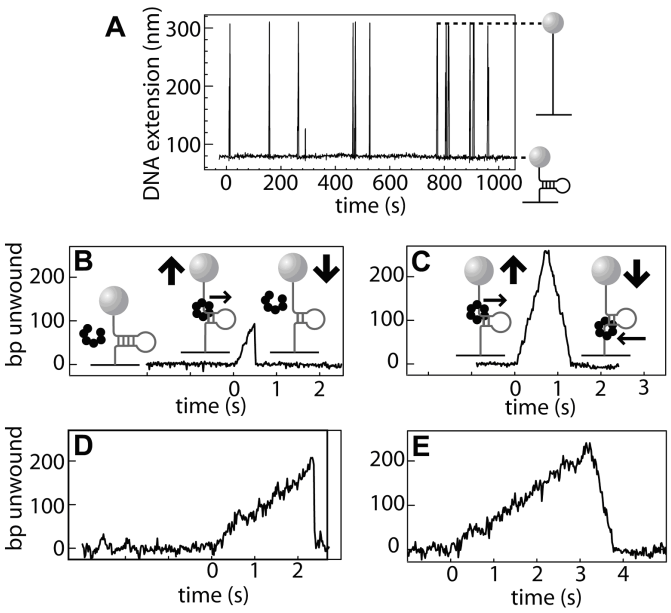

Figure 9: Gp41 unwinds the hairpin substrate in bursts. A) Typical recording of the molecule extension versus time over 20 minutes. Most of the time the hairpin is closed but the helicase is active in short bursts. This signal demonstrate that we are in a single molecule regime. B), C), D), E) close view on the unwinding events. Two kind of events are seen: some with fast falling edge B) and D) and those with slower falling edge. B) and C) are recorded in saturating ATP conditions whereas D) and E) are recorded in condition where ATP is limited resulting in a decreased enzyme rate.

5.1 gp41 unwinding rate measurement

As gp41 and ATP are added into the chamber, we observe short events displaying a transient increase of DNA extension (Fig. 9A)). Between these events, the measured length of the DNA molecule corresponds to the folded state of the hairpin. The slope of the DNA extension time trace during these events (i.e. the unwinding velocity) depends on the ATP concentration (see below). Thus these events result from helicase-catalyzed transient unwinding of the duplex. The time duration of each event is much shorter than the time between events, which guarantees that each event results from the activity of a single helicase complex. The length increase (in nm) we observe can be readily translated into base pairs (bp) at a given force using the measured ssDNA extension vs. force curve 5. This conversion factor is calibrated against the full length of the hairpin, measured as the maximal length of the unwinding events.

Two types of events are observed. The first type consists of a slowly rising edge followed by a rapidly falling edge (Fig. 9B) and C)). The length of these events is variable, distributed between zero and full DNA extension. In contrast with the ATP-dependent slope of the rising edge, the falling edge displays a steep, ATP-independent slope. This means that whereas the rising edge is gp41-controlled, the falling edge is not. As a consequence, the rising edge must correspond to gp41 unwinding the duplex, whereas the falling edge must correspond to the spontaneous re-annealing of the two strands. It is highly unlikely that the two strands re-hybridize around the helicase. We therefore conclude that the first type of event corresponds to gp41 unwinding the duplex, then dissociating from its DNA substrate, allowing the two DNA strands to re-anneal, refolding the hairpin completely.

The second type of event displays a slowly rising edge until the maximum DNA extension (i.e. fully unwound hairpin) followed by a slowly falling edge (Fig. Fig. 9D) and E)). These events all display full-length unwinding of the duplex. Both the rising and falling rates are dependent on the ATP concentration (although they are not necessary equal, see Fig. 9E)). The slowly rising edge displays the same slope as the rising edge in the first type of event. We therefore conclude that it corresponds to gp41 unwinding the entire duplex. The falling edge must also correspond to gp41 activity because it is ATP dependent as well. It is highly unlikely that the falling edge is due to the presence of a second helicase since the probability of coincident binding of two helicases at low concentration is negligible, or that the helicase switches directionality at the center of the hairpin (previous experiments have shown that gp41 translocates with a $5'$ to $3'$ polarity [31]). It is also unlikely that gp41 could switch strands as reported for other helicases [34, 35], expect such events to occur randomly during unwinding and not only in situations with a fully unfolded hairpin. We therefore conclude that this type of event corresponds to the helicase unwinding the entire duplex and then translocating further on the ssDNA, thus blocking the spontaneous, rapid rehybridization of the two separated strands. As the helicase moves on the ssDNA, the fork is able to slowly close in its wake. Thus, the falling edge corresponds to the gp41 translocation-limited rezipping of the opened hairpin.

The unwinding rate v_U can be measured from the slope of the rising edge. We define the rezipping rate v_Z as the slope of the slowly falling edge. The rezipping velocity is ATP-concentration dependent (typically a few 100 bp/s) and can be readily distinguished from the fast, ATP-concentration independent spontaneous rehybridization rate (typically a few 1000 bp/s). Whereas the unwinding rate increases with increasing force, the rezipping rate does not depend on the applied force (compare Fig. 9B vs. 9D; Fig. 9C vs. 9E).

5.2 gp41 rezipping rate is equal to its ssDNA translocation rate

During the rezipping phase, the enzyme translocates on ssDNA, while the fork closes in its wake. Is this situation different from gp41 translocating alone on ssDNA? The fork closing behind the enzyme might alter the enzyme translocation rate in two possible, but not mutually exclusive ways: first, the pairing energy gained by the fork while it is closing might provide an effective driving force to the translocating helicase; and second, the mere presence of the fork in the vicinity of gp41 might affect its velocity.

We addressed the first point by measuring the gp41 rezipping rate v_Z as a

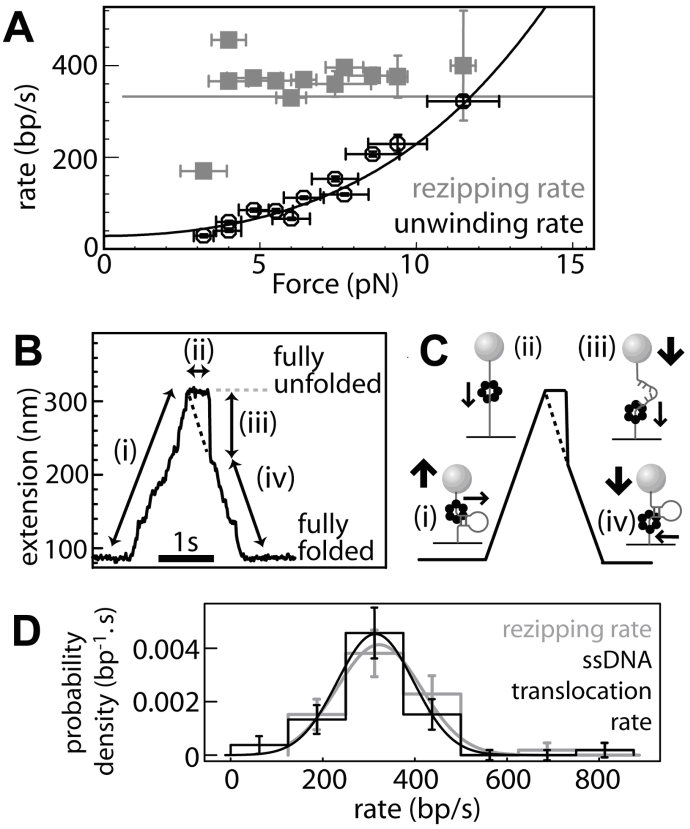

Figure 10: Third type of gp41 unwinding events occurring when the force is approaching the unzipping force. In this situation, once the hairpin is open, it refolds after some latency (typically one second). During that time the gp41 helicase travels on single stranded DNA. When the hairpin finally refolds the refolding fork progress very rapidly until it bumps in the helicase. Then, the hairpin closing is controlled by gp41 translocation. We find that the gp41 rezipping rate equals its ssDNA translocation rate.

function of force. At low force ($F \approx 3$pN), the folded hairpin is highly stable; therefore, the potential driving force exerted by the fork should be the greatest. In contrast, when approaching the mechanical unfolding transition ($F \approx 12$ pN), the effective driving force should approach zero since the paired and unpaired forms of the hairpin are equally stable at the transition. Therefore, one would expect significant changes in the driving force between 3 and 12 pN that should reflect on v_Z. We find that the rezipping rate v_Z does not depend on the force exerted (compare Fig. 9C and 9E; Fig. 10A). Therefore, we conclude that the pushing action of the closing fork due to the energy gain upon base-pairing is negligible.

To address the influence of the presence of the fork behind gp41, we performed the following experiment: we increased the force to a value close to the unfolding transition. In this regime, the folded hairpin is stable on the timescale of the experiment; however, if previously unfolded, the spontaneous rehybridization of the two strands does not take place immediately, but after a fraction of second. We then recorded gp41 unwinding events. In addition to the two main types of events described above, we observed a third type (Fig. 10B). After a careful evaluation of the other potential interpretations for these events, we dismiss them and conclude that

these events correspond to a single enzyme unwinding dsDNA (i) and continuing to translocate on ssDNA, first without any fork behind it (ii and iii), then with the fork closing in its wake (iv) (Fig. 10C). We can measure the rezipping rate during these events as the slope of the extension time trace during phase (iv). In contrast, the translocation of the enzyme on the stretched ssDNA does not change its extension; however, we can estimate this rate as the ratio of the distance traveled divided by the time the hairpin remains unfolded ($\delta L/\delta t$ on Fig. 10C, (ii)/(iii)). We then compare the rates of translocation on ssDNA with or without a fork closing behind the helicase. In the conditions explored ($F > 7$ pN; 0.5 mM $\leq$ [ATP] $\leq$ 5 mM) the mean rates are similar (Fig. 10D) differing by only 5% (S.D. 20 % N = 10 events).

We therefore conclude that the rezipping rate is equal to the ssDNA translocation rate. As a consequence, we can measure the dsDNA unwinding rate and the ssDNA translocation rate under the exact same conditions to quantify how gp41 slows down while unwinding dsDNA as compared to when it translocates on ssDNA. These measurements, performed as a function of force and ATP concentration, provide us with a set of data amenable to test various helicase mechanisms.

5.3 ssDNA translocation does not involve cooperative ATP hydrolysis

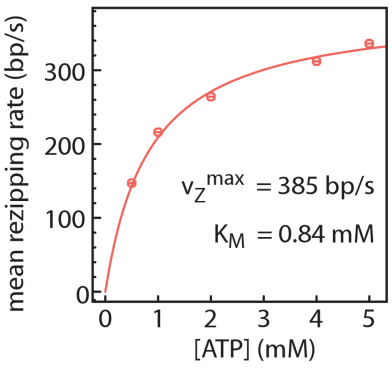

Figure 11: The rezipping rate versus the concentration of [ATP] follows a first order Michaeli-Menten law. The rezipping rate increase linearly with the ATP concentration at low value it saturates when [ATP] approaches the mM concentration. This rezipping rate is independent of the force applied on the hairpin.

We first characterized the ssDNA translocation rate dependency on ATP. For each ATP concentration, we obtained the ssDNA translocation rate as the average of the force-independent rezipping rates (Fig. 3). The resulting ssDNA translocation velocity vs. ATP concentration curve was fit to the Michaelis-Menten equation, $< |vZ| >= v_Z max[ATP]/(Km + [ATP])$, with a maximum velocity ($v_Z max$) of 400$\pm$10 bp/s and Km of 1.1$\pm$0.1 mM. The observed non-sigmoidal kinetics rule out a translocation mechanism involving simultaneous ATP hydrolysis by the six helicase monomers, but cannot distinguish between independent or cooperative ATP binding. Based on this result, we have modeled gp41 translocation on ssDNA involving a reversible ATP binding step followed by an irreversible translocation event (Fig. 13A)).

5.4 gp41 a passive helicase

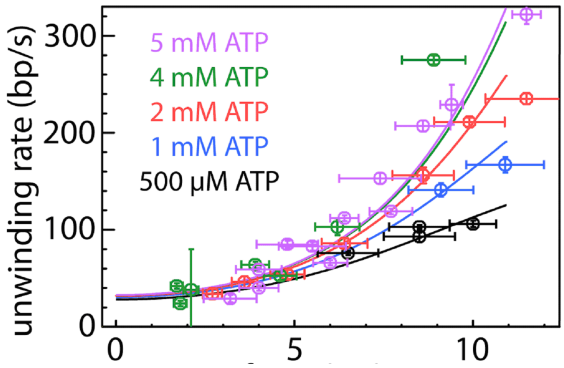

Figure 12: The unzipping rate of the gp41 helicase versus force at various [ATP] concentration. This rate corresponds to the velocity of the helicase when unwinding the dsDNA. Notice that this rate depends very strongly on the force applied to the hairpin as well as the [ATP] concentration. A fit to the force dependence is compatible with an exponential suggesting that the rate may be described by an Arrhenius process.

Next, we measured the dsDNA unwinding rate v_U as a function of applied force and ATP (Fig. 12). The unwinding rate increases continuously with increasing force and ATP concentration. The maximum unwinding velocity measured at the critical force where the hairpin is marginally stable ($F \approx 12$pN) agrees with the translocation velocity on ssDNA (Fig. 10A) at the same ATP concentration.

We have represented these results using a simple global model for helicase activity on ssDNA and dsDNA [36]. We assume that the enzyme first binds ATP reversibly and that translocation is coupled to ATP hydrolysis. In the case of ssDNA translocation, the enzyme step size is n bp and occurs with rate k_+ (Fig. 13A)). In the case of dsDNA unwinding (Fig. (Fig. 13B)), the fork must open by n bp prior to translocation. The kinetics of fork opening/closing depend on the force exerted to open the hairpin and the active/passive character of the helicase. Finally, translocation by n bases takes place with the same rate k_+ as on ssDNA.

The active/passive nature of the helicase is introduced in to the model through the fork opening and closing rates, α and β respectively, following a recent model [37, 38]. Briefly, if the enzyme is passive, the opening/closing kinetics of the fork are unaffected by the presence of the helicase. In contrast, an active helicase directly destabilizes the double helix. As a result, α and β depend on the position of the enzyme relative to the fork. When the enzyme is at the fork, the opening step is favored over the closing one. This is modeled by lowering the energy of unpairing at the fork (i.e. the equilibrium constant α/β) by a fixed amount when the enzyme is within n bp of the fork. The amount of energy devoted by the enzyme to the destabilization of the junction constitutes a measure of the active character of the enzyme. We have assumed that the base pairing energy is homogeneous, thus neglecting sequence effects. To preserve generality. Using a simple version of the model assuming that destabilization by the helicase occurs on the range of its step size and neglecting activation barrier position effects. We have been able to determine that gp41 mechanism was mostly passive [36], the energy of the helicase involved in fork destabilization being equal to 0.15 k_BT while that involve in melting one base pair

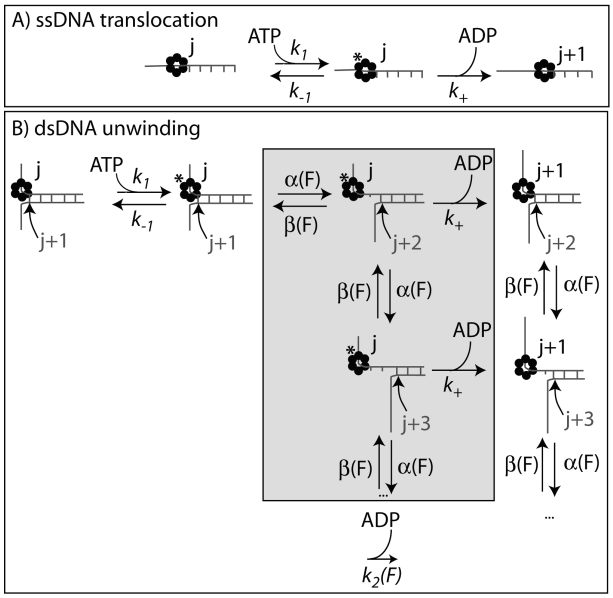

Figure 13: Models describing the various states involve during the gp41 helicase translocation. A) when the substrate is only ssDNA, the motion is only dependent on the ATP binding and hydrolysis. B) when unwinding a real dsDNA the mechanism involves more states. In the passive model, after ATP binding, the spontaneous opening of the DNA fork upon thermal fluctuations offers to the helicase opportunity to quickly move forward. In the active model the helicase destabilizes the DNA fork and opens it by melting the base pairing of the nucleotide j+1 at the fork. All those process may be described by appropriate chemical rate constant k_i

is $\approx 2k_BT$.

6 Behaviour of the primosome: coupling activity of the helicase and the primase

Here we focus on the study of the primosome and the interactions between the helicase and primase during primer synthesis. The primosome is known to play a crucial role in coupling leading and lagging strand DNA synthesis: the helicase unwinds the DNA for the leading strand holoenzyme and the primase repetitively primes the lagging strand for Okazaki fragment synthesis by the lagging strand holoenzyme. The two proteins clearly form a complex since both proteins enhance the activity of the other [25, 39, 40]; however the helicase translocates 5' to 3' on the lagging strand and the primase must travel in the opposite direction (3' to 5') in order to synthesize an RNA primer.

6.1 Models of primosome behavior during primer synthesis

Three different model are possible for the coupling activities of the helicase and the primase (see Fig 14). In the pausing model the helicase stops to allow the primase to synthesize a primer. The unwinding and the leading strand synthesis are then interrupted each time that a new primer is synthesized. This is the behavior observed in the T7 bacteriophage replisome [41]. In the disassembly model one of more subunits of primase dissociate from the hexameric helicase during priming,

allowing the unwinding and leading strand synthesis occurs continuously. However new primase subunits might need to be recruited at each cycle of Okazaki fragment synthesis. Trapping experiments with an inactive primase protein have shown that the gp61 primase is distributive suggesting that in T4 system a new primase subunit may be recruited with initiation of each Okazaki fragment [42]. Finally, in the looping model the primosome remains intact during priming by looping the DNA that is being unwound by the helicase. After priming the primosome can transfer the primer directly or indirectly to the lagging strand polymerase and release the lagging strand loop. This looping mechanism allows the helicase continuously unwind the DNA but without dissociating from the primase.

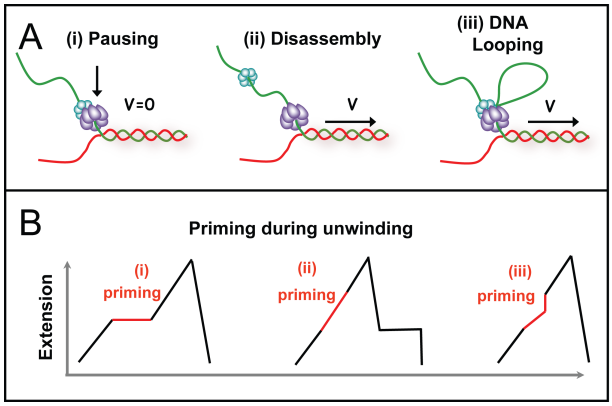

Figure 14: (A) Schematic representation of three possible models for helicase and primase interaction during primer synthesis: (i) in the pausing model the helicase and primase temporarily stop translocating during priming; (ii) in the disassembly model the primase dissociates from the helicase to synthesis a primer while the helicase continues unwinding DNA; (iii) in the DNA looping model the primosome remains intact and DNA unwound during priming forms a loop. (B) Schematic representation of the real-time DNA extension traces expected for each of the three models.

6.2 Two priming mechanisms

We have performed experiments with both the gp41 and gp61 primase to investigate how these two enzymes couple their activities and motions. In absence of rNTPs (situation in which priming cannot occur), the results are indistinguishable from those obtained with the helicase alone (see Fig 15): the enzymatic events start with a rising edge that is associated to the unwinding activity and end with a falling edge corresponding to the ssDNA translocation activity followed by the rezipping of the hairpin. The unwinding and translocation velocity measured respectively from the unwinding and rezipping phases coincides with those measured in the experiments with the helicase alone. In contrast, in presence of rNTPs the enzymatic events present two new features: (i) the rezipping signal is strongly altered by the presence of blocks; (ii) once in a while a sudden extension increase (jump) is observed during the unwinding edge (see Fig 15). These new features, blocks and jumps, are only observed in presence of rNTPs and their frequency depends on the rNTP concentration [43]. As a result, the observed blocks during rezipping and jumps during unwinding are signatures of the priming activity of the primosome.

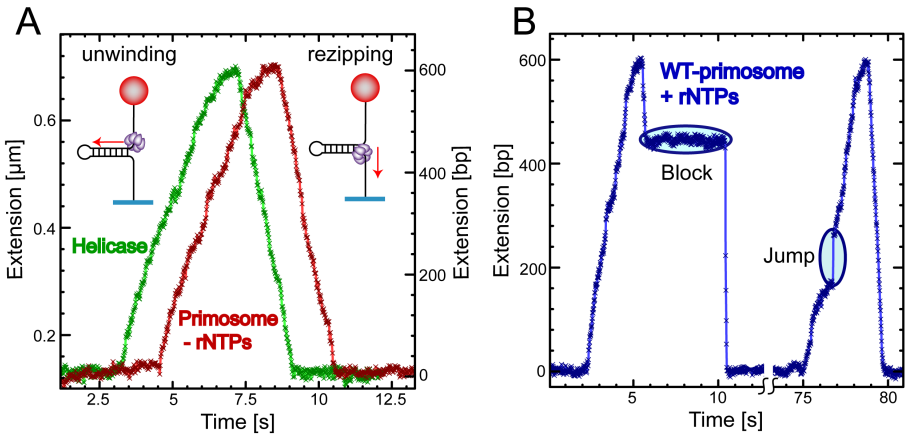

Figure 15: (A) Experimental traces corresponding to the gp41 helicase activity (green) and the wild-type primosome activity (red) on the S1 hairpin in the absence of rNTPs (B) Examples of two new features, blocks in hairpin reannealing and jumps in extension during unwinding, observed in experimental traces from wild-type primosome activity on 600bps hairpin in the presence of 1 mM rNTPs.

Using DNA substrates with special designed sequences (showing available recognition priming sites only along one strand) we have established that priming can only occur during unwinding in our experimental configuration [43]. Probably priming during rezipping is inhibited by the reannealing of the hairpin behind the primosome, a situation which is also unnatural in a normal DNA replication fork where the DNA unwound by the helicase would be coated with ssDNA binding protein gp32. Therefore, the two different priming signatures (jumps during unwinding and block during rezipping) we observe are likely the result of two different priming mechanisms being employed by the primosome.

6.3 Primosome does not pause but disassembles

If the T4 primosome stopped during priming this would result in the presence of pauses in the DNA unwinding traces. Long periods of no change in the DNA extension during unwinding were rare and their frequency was independent of the rNTP concentration showing that they were not a signature of the priming activity. Moreover, these pauses occurred at the GC rich regions suggesting that they corresponded to the slowing down of the helicase when encountering regions of high DNA stability. We then conclude that the T4 primosome does not pause during priming. In contrast, when rNTPs were present long periods of no change in the DNA extension were frequently observed during the rezipping phase of the experimental traces. The frequency of such blocks increased upon rNTP concentration and their position along the sequence was correlated with the position of the priming sites in the lagging strand available during unwinding (see Fig 16). Overall these results show that the blocks observed during the rezipping phase are related to the priming activity during unwinding. Moreover the presence of blocks is predicted by the disassembly model (see Fig 14). In that model during priming the primase dissociates from the helicase without altering the unwinding activity. The synthesized primer and/or some primase units might remain bound to the DNA blocking the reannealing of

the hairpin during the rezipping phase (see Fig 16). The blocks in DNA rehybridization could be caused by the pentaribonucleotide primer itself, dissociated primase subunit(s), or a complex of the primase subunit(s) with the primer bound to the DNA hairpin. Several experiments were preformed to investigate the nature of these blocks. Results suggest that blocks are generated by the primer/primase complex [43].

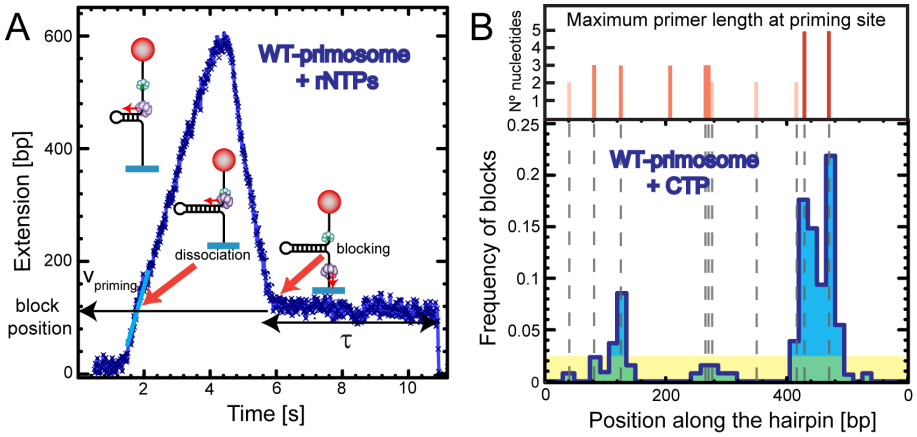

Figure 16: (A) Experimental trace displaying characteristics of the primosome disassembly model. The unwinding velocity during primer synthesis, the position of the priming site, and the lifetime of the block in hairpin rehybridization are indicated. (B) Distribution of blocks plotted against the corresponding position along the hairpin substrate measured with wild-type primosome in the presence of CTP and ATP from 345 blocking events. The location of the priming sites available on the 5' strand are indicated by dashed gray lines. The uniform light yellow distribution represents primase binding randomly along the DNA hairpin and not specifically at priming sites. The maximum primer length that may be synthesized at each priming site at the give rNTP conditions is shown in the upper panel.

6.4 Primosome activity by DNA looping

The other type of priming events, jumps during unwinding, can not be explained neither by the disassembly nor by the pausing model, but by the DNA looping model. In this model, during priming the helicase continuously unwinds the DNA without dissociating from the primase. The unwound DNA in the lagging strand is then looped and released once priming is over. The release of a ssDNA loop that is formed during priming should provide a sudden increase of the molecular extension (see Fig 14B). This signature is observed on the second type of priming events (see Fig 15), revealing that priming can be carried out not only by primosome disassembly (which generates blocks during rezipping) but also by DNA looping (identified with extension jumps). During loop formation only one of the two strands of the unwound DNA contributes to the elongation of the measured molecular extension (see Fig 17). Accordingly the apparent DNA unwinding velocity immediately prior to a sudden increase in the DNA extension is smaller than the DNA unwinding velocity when no looping occurs (see Fig 17A). In particular its mean value is one-half of the mean DNA unwinding velocity [43]. This indicates that the primosome continues to unwind the DNA at a constant rate regardless of whether it is synthesizing a primer

and consequently forming a DNA loop. As shown in Fig 17B, the size of the loop follows a Gaussian distribution with a mean value of 250 nucleotides. Considering a mean unwinding velocity of 220 bp/s, the average time involved in loop formation and release is about 1 s. This value is consistent with the priming rate of 1 primer per second per replisome, which has been measured in bulk experiments [44].

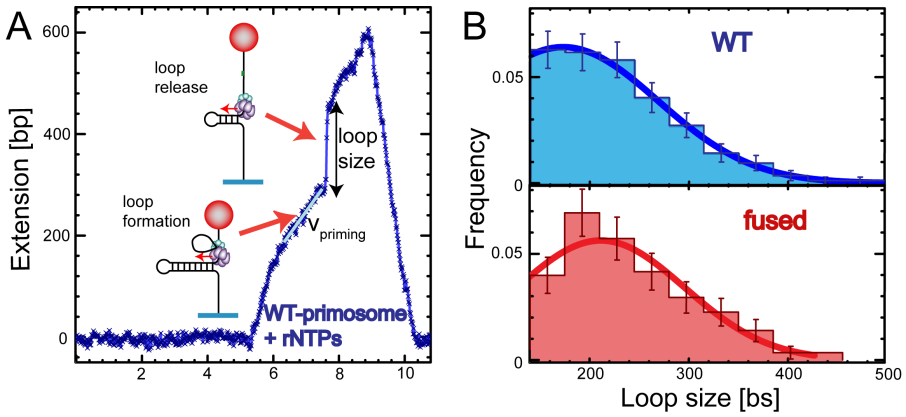

Figure 17: Experimental trace displaying characteristics of the DNA looping model. The unwinding velocity during primer synthesis and the loop size are indicated. Distribution of the DNA loop size for wild-type primosome (blue) and fused primosome (red) from 71 and 42 priming events involving loop formation, respectively. A minimum loop size of 140 nucleotides was used as a cutoff. Histograms are fit to a Gaussian function yielding a mean DNA loop size of 170 20 and 210 20 nucleotides for wild-type and fused primosome, respectively.

Priming by DNA looping is infrequent, less than ten times less frequent than priming by primosome disassembly (see Fig 18B). We then conclude that the primase processivity is very low in our experimental conditions: the primase mostly dissociates from the helicase during priming and hence the primosome rarely remains intact. In this latter case, disassembly of the primosome is prevented by DNA looping. Interestingly experiments with a primosome consisting of a fused primase-helicase protein [43] works exclusively through a DNA looping model. In these experiments, in absence of rNTPs, the detected activity is similar to the wild-type-gp41 activity. As rNTPs are added, the enzymatic events show the presence of jumps in extension during the unwinding phase (see Fig 18A). In contrast to the wild-type experiments, the loops are frequently observed, the frequency being ten times larger than in the wild-type case (see Fig 18B).

6.5 Force does not hamper loop formation

When a pulling force is applied to stretch DNA, the primosome must work against it to form a loop during priming. We have performed low force experiments in order to investigate whether the applied force is preventing loop formation and/or favoring primosome disassembly. At low pulling force the signal to noise ratio is lower because the extension of ssDNA is short and the fluctuations in extension are large. 5 pN is the lowest force to which we can work and keep a good spatial resolution. Comparison between the results obtained at 9pN and 5pN with the wild-type-primosome show that the force does significantly affect neither the frequency of loop formation nor the frequency of the primase dissociation [43]. These results

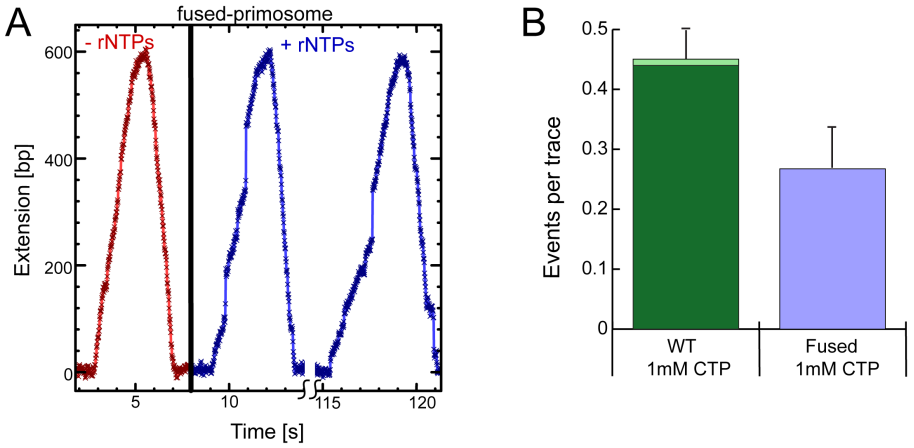

Figure 18: (A) Experimental traces corresponding to the fused primosome activity in absence (red) and presence of rNTPs (blue). (B) Stacked histogram of the frequency of blocks in hairpin reannealing (dark green or blue) and jumps in extension during unwinding (light green or blue) measured in experiments with wild-type (green) and fused (blue) primosome in the presence of CTP on a 600 bps hairpin. The frequency is calculated as the number of events per enzymatic trace, where an enzymatic trace is defined as a trace demonstrating complete unwinding and rezipping. The number of enzymatic traces analyzed for each condition is 447 and 169 in order.

show that primosome disassemble and subsequent low primase processivity are not an artifact of our experimental approach but they rather are an intrinsic property of the T4 wild-type-primosome. However, as suggested by recent bulk experiments [45], in the context of the full replisome other proteins might control the partitioning of these two mechanisms preventing primosome disassembly thereby increasing primase processivity.

7 DNA synthesis

The gp43 is a monomeric polymerase that catalyzes the template-directed incorporation of dNTPs into the nascent DNA in both leading and lagging strand synthesis. However, leading and lagging strand synthesis require the presence of other replisomal proteins. In particular, only gp43 and gp41 are needed for leading strand synthesis [32] whereas the full replisome must be assembled for lagging strand synthesis. Nevertheless, the polymerase can perform chain elongation on ssDNA templates without gp41. Gp43 alone is not very efficient, but together with the three T4 polymerase accessory proteins (gp44/62 and gp45) becomes a highly processive enzyme [46]. The complex formed by the polymerase and the gp45 clamp, called the holoenzyme, is assembled and loaded by the gp44/62 clamp-loader [22, 23]. The holoenzyme alone can also carry out strand displacement activity on dsDNA templates but its leading strand synthesis rate (10bp/s) is about 30 times slower than when gp41 is present [32, 33].

7.1 Measuring strand displacement synthesis and chain extension activity on ssDNA

The DNA substrates to study polymerase activity are the same used for the helicase and primosome assays: DNA hairpins of different lengths (from 1,2 to 7Kbp) aiming to mimic a replication fork. Since gp43 requires a DNA or RNA primer to start the polymerization reaction, the different DNA hairpins have a dsDNA tail at the 3' end (see Fig 19A). The latter can be used as a primer allowing the polymerase to initiate leading strand synthesis. Interestingly, these DNA substrates allow us to study not only strand displacement polymerase activity but also the activity on ssDNA. The first part of the synthesis corresponds to strand displacement activity, since the polymerase needs to displace the lagging strand in order to extend the dsDNA tail primer. Moreover, in absence of lagging strand synthesis a second phase is possible. The latter corresponds to the polymerase reaching the end of the hairpin and copying the rest of the ssDNA substrate (see Fig 19B). The strand displacement phase should produce an increase in the substrate extension, corresponding to the gain of one bp on the 3' tail and one ssDNA base on the 5' tail for each base added. The second phase, corresponding to the conversion of ssDNA to dsDNA, might have a different signature depending on the force applied. ssDNA is longer than dsDNA above 5pN and shorter below (see Fig 5) . Therefore the polymerase activity on ssDNA should result on an increase on extension at high forces (above 5pN) and a decrease on extension at low forces (below 5pN), as shown in Fig 19B.

7.2 Polymerase and holoenzyme activities

By injecting gp43 and NTPs into the chamber some polymerase activity could be detected at high enough forces (higher than 7pN) (see green trace in Fig 20). By using the previously measured elasticity of ssDNA and dsDNA molecules (see Fig 5) we can estimate the rates of DNA synthesis. The polymerization rate either during strand displacement or during primer extension on ssDNA was much lower than the replication rate of the full replisome measured in bulk experiments [32, 33]. Moreover long pauses were frequently observed, suggesting that the processivity of the enzyme was very low (few bases). In the presence of the clamp and clamp loader the rates measured in the two phases of polymerization (strand displacement and synthesis on ssDNA template) were much higher, but still lower than the 300-400bp/s expected for replication fork advance [32, 33]. The rate during strand displacement was extremely sensitive to the value of the applied force, its value changing by two orders of magnitude when varying the force from 10pN to 4pN (see blue traces in Fig 20).

The work required to a open a bp at a given force F is given by $W = \Delta G - \int_0^F x(f)df$, where ΔG is the base pair energy and $x(f)$ is the extension of 2 nucleotides of ssDNA stretched by a force f. The work W corresponds to the energy barrier that the polymerase needs to overcome for incorporating one base during strand displacement activity. Accordingly we find that higher forces results on larger polymerization rates. Thus we conclude that the force applied to the ends of the molecule helps the progress of the polymerase by destabilizing the base pair at the fork and decreasing the energy barrier for polymerase advance. On the contrary, the rate of polymerase activity on ssDNA was force-independent at the range of forces studied (between 4pN and 16pN) .

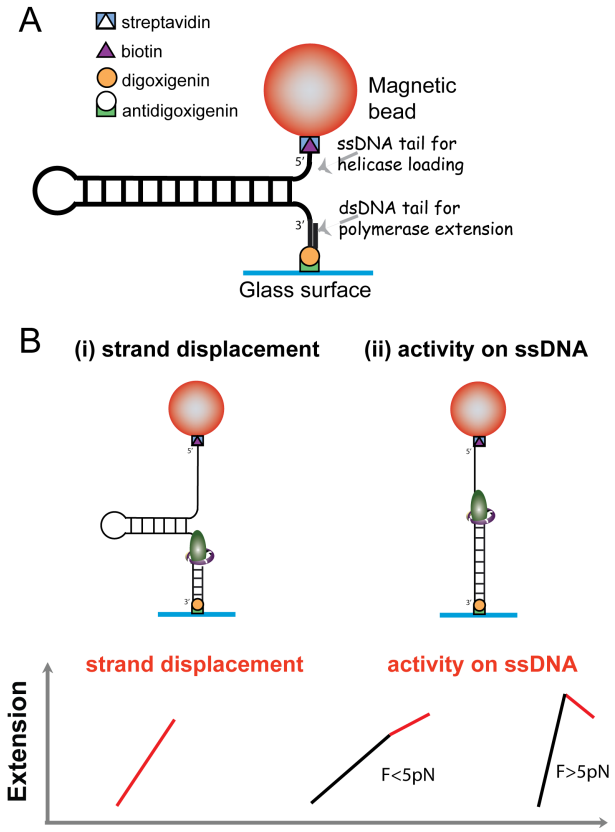

Figure 19: (A) Schematic representation of the DNA hairpin substrate used in polymerase assays, having a 5'-biotinylated ssDNA tail, and a 3'-digoxigenin labeled dsDNA tail. The DNA hairpin is specifically attached to the magnetic bead coated with streptavidin and to the glass surface treated with anti-digoxigenin antibody. (B) Two phases of polymerase activity can be studied. The first phase corresponds to the strand displacement activity and can be identified with the initial increase in DNA extension. The second phase corresponds to the DNA chain extension on ssDNA and it can be identified with the final increase (decrease) in DNA length at forces larger (smaller) than 5pN.

7.3 Leading strand synthesis: coupling helicase and polymerase activities

Coupled helicase and polymerase activity to perform leading strand synthesis was observed in presence of holoenzyme, helicase, ATP and dNTPs (see Fig 21A). In general better activity was observed at low forces (between 2pN and 5pN). At high forces, most of the time the two enzymes worked in uncoupled mode (traces show separate helicase and polymerase activity, see Fig 21B). As expected the polymerization rate observed in the coupled gp41-gp43 activity was independent of the applied force and agrees with the values of the replication rate measured in bulk assays [32, 33]. Interestingly, at the range of forces where coupled activity is observed (between 2 and 7pN) the measured polymerization rate is higher than that of the helicase or the holoenzyme alone. Moreover pauses are observed very rarely suggesting that the processivity of the gp41-gp43 complex is very high (larger than 1kbp). In other words, the coupling between these two enzymes (direct or indirect) enhances both helicase and polymerase activities.

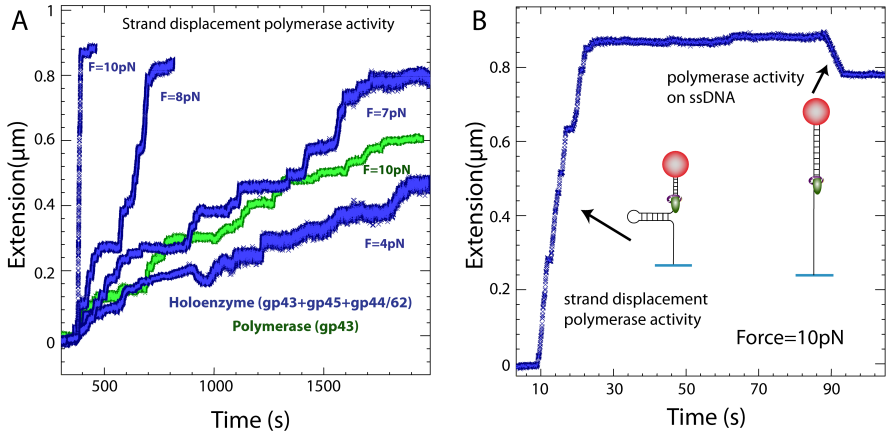

Figure 20: (A) Experimental traces corresponding to the strand displacement activity of the gp43 polymerase (green) and holoenzyme (blue) in presence of 500 μM NTPs. Results for the gp43 polymerase are obtained at 10pN of applied force. Different trajectories for the holoenzyme correspond at different forces, ranging from 4pN to 10pN. (B) Trace corresponding to the full synthesis of the DNA substrate, containing the strand displacement phase and the ssDNA activity phase, catalyzed by the holoenzyme at 10pN of applied force.

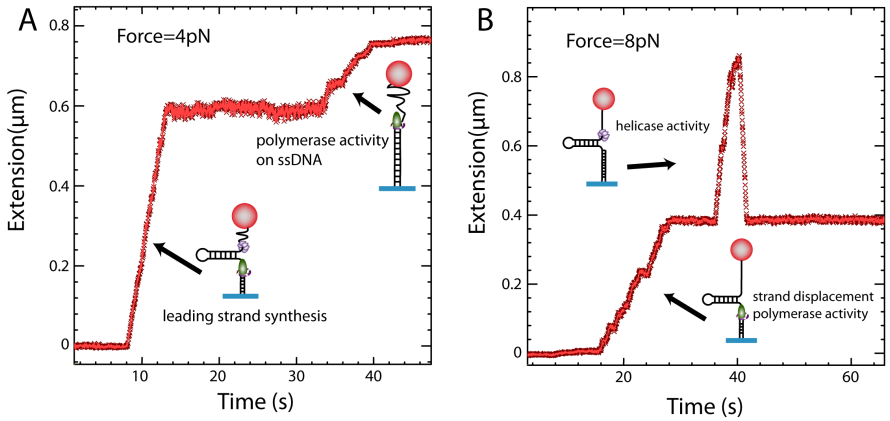

Figure 21: (A) Experimental trace corresponding to the leading strand synthesis carry out by the helicase and holoenzyme in presence of ATP and NTPs and at 4pN of applied force. (B) Experimental trace showing the uncoupled activity of the helicase and polymerase observed at high forces.

8 Conclusions

DNA replication is a complex process involving a large number of proteins. In this paper, we have used magnetic tweezers to investigate the replisome of the T4 bacteriophage. The T4 replisome is formed by 8 different proteins that work in a very coordinated fashion in order to copy the T4 genome at high speed (300bp/s) and with a high processivity (larger than the size of the genome, 180Kbp). Our approach does not allow to directly visualize the different proteins of the replisome but only to measure their overall activity as a change in the conformation of the DNA molecule that is being replicated. How from these measurements one can obtain information

about the functioning of the replisome? Can one investigate the interaction between the different replisomal proteins that allow the progress of the replication fork and coordinate the DNA synthesis in the leading and lagging strands? Our strategy consists of first characterizing the activities of the different replisomal proteins separately. Next the behaviour of sub-assemblies of different parts of the replisome is investigated. In this way we attempt to build up the full replisome by increasing, step by step, the complexity of the system studied.

The activities of the gp41 helicase and the gp43 polymerase alone on a DNA hairpin have been extensively characterized. Both enzymes work fast and processively only at high force. In contrast at low force their activity is more than 10 times slower than the rate of movement of the replication fork as measured in bulk assays [32, 33]. Comparison of the experimental results with models have shown that gp41 unwinds DNA as a passive helicase [36]; that is it does not actively destabilizes the double helix but it works as a ssDNA translocase trapping the spontaneous opening fluctuations of the fork (35). These results show that both helicase and polymerase need other replisomal partners in order to reach its full speed.

We have next studied the primosome, formed by the helicase and primase, which is responsible for DNA unwinding and initiation of Okazaki fragments. Our results show that the T4 primosome continuously unwinds the DNA duplex while allowing for primer synthesis through a primosome disassembly or a DNA looping mechanism[43]. The activity of the holoenzyme, responsible for the processive DNA polymerization, can be also be observed when the polymerase, clamp and clamp loader are studied together. Their speed and processivity are larger than those of the polymerase alone but still much lower (specially at low force) than those expected by the full replisome. Interestingly efficient leading strand synthesis is observed when the holoenzyme and helicase are bring together at low force. The coupling between polymerase and helicase enhances both unwinding and polymerization activities, since the measured rate of synthesis at low forces is much higher than either the unwinding rate of the helicase or the polymerization rate of the holoenzyme alone. Addition of the primase and the single-stranded binding protein might allow to form the full replisome and study the coordination between leading and lagging strand synthesis.

In this paper we have seen how one of the new tools of single molecule manipulation (magnetic tweezers) can be applied to the study the enzymes involved in the DNA replication. The level of precision and detail of these experiments is often unmatched by bulk assays. These techniques allow one to generalize to a large class of enzymes the approach applied successfully and for many years to the study of ion channels. We have hereby only described one aspect of recent single molecule studies, those involving their manipulation. Another equally exciting and powerful approach is using single molecule fluorescence and fluorescence resonant energy transfer (FRET) to monitor the motion of a single enzyme on its substrate[47] and its internal conformational changes[48] with nanometer accuracy and millisecond time resolution[49] . Combining both approaches [50] will provide new opportunities for single molecule enzymology, where all (or most) of the parameters characteristic of a single molecular motor will be measured simultaneously (its rate, processivity, step-size, work done and number of ATP molecules consumed per cycle[51]). The characterization of the dynamic feature of an enzyme together with its static crystallographic data should provide an (almost) complete picture of its mechanism.

9 Acknowledgments

We thank our collaborators on the presented works: M.M. Spiering, S.J. Benkovic. This work was supported by grants from HFSP, ANR, and the EEC under the "BioNanoSwitch" program.

References

[1] C. Bustamante, S. B. Smith, J. Liphardt and D. Smith, *Single-molecule studies of DNA mechanics*, Curr. Op. Structural Biology **10** (2000), 279–285.

[2] T.R. Strick, M.-N. Dessinges, G. Charvin, N.H. Dekker, J.-F. Allemand, D. Bensimon, and V. Croquette, *Stretching of macromolecules and proteins*, Rep. Prog. Phys. **66** (2003), 1–45.

[3] G. Lia, D. Bensimon, V. Croquette, J.F. Allemand, D. Dunlap, D.E.A. Lewis, S. Adhya, and L. Finzi, *Supercoiling and denaturation in gal repressor-heat unstable nucleoid protein (hu)-mediated dna looping*, Proc. Natl. Acad. Sci. (USA) **100** (2003), 11373–11377.

[4] J. Liphardt, B. Onoa, S. B. Smith, I. Tinoco Jr., and C. Bustamante, *Reversible unfolding of single RNA molecules by mechanical force*, Science **292** (2001), 733–737.

[5] J.F. Marko and E.D. Siggia, *Driving proteins off DNA using applied tension*, Biophys. J. **73** (1997), 2173–2178.

[6] A. Engel and H.E. Gaub and D.J. Müller, *Atomic force microscopy: A forceful way with single molecules*, Curr. Biol. **9** (1999), pR133-R136.

[7] E. Evans and K. Ritchie, *Dynamic Strength of Molecular Adhesion Bonds*, Biophysical Journal **72** (1997), p1541–1555.

[8] P. Cluzel, A. Lebrun, C. Heller, R. Lavery, J.-L. Viovy, D. Chatenay and F. Caron, *DNA: an extensible molecule*, Science **271** (1996), p792–794.

[9] S.B. Smith, L. Finzi and C. Bustamante, *Direct Mechanical Measurements of the Elasticity of Single DNA Molecules by using Magnetic Beads*, Science **258** (1992), p1122–1126.

[10] S. Chu, *Laser manipulation of atoms and particles*, Science **253** (1991), p861–866.

[11] J.-F. Allemand, T. Strick, V. Croquette, and D. Bensimon, *Twisting and stretching single dna molecules*, Prog. Biophys. Molec. Biol. **74** (2000), 115–140.

[12] F. Gittes and C.F. Schmidt, *Signals and noise in micromechanical measurements*, Methods in Cell Biology **55** (1998), 129–156.

[13] J.-F. Allemand, D. Bensimon, R. Lavery, and V. Croquette, *Stretched and overwound DNA form a Pauling-like structure with exposed bases*, Proc. Natl. Acad. Sci. USA **95** (1998), 14152–14157.

[14] M.-N. Dessinges, B. Maier, Y. Zhang, M. Peliti, D. Bensimon, and V. Croquette, *Stretching ssdna, a model polyelectrolyte*, Phys. Rev. Lett. **89** (2002), 248102.

[15] J.F. Marko and E. Siggia, *Statistical mechanics of supercoiled DNA*, Phys. Rev. E **52(3)** (1995), 2912–2938.

[16] C. Bouchiat, M.D. Wang, S. M. Block, J.-F. Allemand, T.R. Strick, and V. Croquette, *Estimating the persitence length of a worm-like chain molecule from force-extension measurements*, Biophys. J. **76** (1999), 409–413.

[17] T. Strick, J.-F. Allemand, D. Bensimon, and V. Croquette, *The behavior of supercoiled DNA*, Biophys. J. **74** (1998), 2016–2028.

[18] C.C. Richardson, Cell **33** (1983), 315–317.

[19] S.P. Bell, and A. Dutta, *DNA replication in eukaryotic cells*, Annu. Rev. Biochem. **71** (2002), 333–374.

[20] S.J. Benkovic, A.M. Valentine, and F. Salinas, *Replisome-mediated DNA replication*, Annu. Rev. Biochem. **70** (2001), 181–208.

[21] C.F. Morris, N.K. Sinha, and B.M. Alberts, *Reconstruction of bacteriophage T4 DNA replication apparatus from purified components: rolling circle replication following de novo chain initiation on a single-stranded circular DNA template*, Proc. Natl. Acad. Sci. USA **72** (1975), 4800–4804.

[22] C.C. Huang, J.E. Hearst, and B.M. Alberts, *Two types of replication proteins increase the rate at which T4 DNA polymerase traverses the helical regions in a single-stranded DNA template*, J. Biol. Chem. **256** (1981), 4087–4094.

[23] B.F. Kaboord, and S.J. Benkovic, *Accessory proteins function as matchmakers in the assembly of the T4 DNA polymerase holoenzyme*, Curr. Biol. **5** (1995), 149–157.

[24] C.C. Liu, and B.M. Alberts, *Characterization of the DNA-dependent GTPase activity of T4 gene 41 protein, an essential component of the T4 bacteriophage DNA replication apparatus*, J. Biol. Chem. **256** (1981), 2813–2820.

[25] D.M. Hinton, and N.G. Nossal, *Bacteriophage T4 DNA primase-helicase. Characterization of oligomer synthesis by T4 61 protein alone and in conjunction with T4 41 protein*, J. Biol. Chem. **262** (1987), 10873–10878.

[26] J. Yang, J. Xi, Z. Zhuang, and S.J. Benkovic, *The oligomeric T4 primase is the functional form during replication*, J. Biol. Chem. **280** (2005), 25416–25423.

[27] P.D. Chastain, 2nd, A.M. Makhov, N.G. Nossal, and J. Griffith, *Architecture of the replication complex and DNA loops at the fork generated by the bacteriophage t4 proteins*, J. Biol. Chem. **278** (2003), 21276–21285.

[28] J. Barry, and B. Alberts, *Purification and characterization of bacteriophage T4 gene 59 protein. A DNA helicase assembly protein involved in DNA replication*, J. Biol. Chem. **269** (1994), 33049–33062.

[29] K.D. Raney, T.E. Carver, and S.J. Benkovic, *Stoichiometry and DNA unwinding by the bacteriophage T4 41:59 helicase*, J. Biol. Chem. **271** (1996), 14074–14081.

[30] F. Dong, E.P. Gogol, P.H. von Hippel, J. Biol. Chem. **270** (1995), 7462–7473.

[31] M. Venkatesan, L.L. Silver, and N.G. Nossal, J. Biol. Chem. **257** (1982), 12426–34.

[32] F. Dong, S.E. Weitzel, P.H. von Hippel, Proc. Natl. Acad. Sci. U S A **93** (1996), 14456–14461.

[33] F. Salinas, and S.J Benkovic, Proc. Natl. Acad. Sci. U S A **97** (2001), 7196–7201.

[34] M.N. Dessinges, T. Lionnet, X.G. Xi, D. Bensimon, and V. Croquette, *Single molecule assay reveals strand switching and enhanced processivity of uvrd*, Proc. Natl. Acad. Sci. U S A **101** (2004), 6439–44.

[35] D. S., L., B. Johnson, B.Y. Smith, S.S. Patel, and M.D. Wang, Cell **129** (2007), 1299–1309.

[36] T. Lionnet, M.M. Spiering, S.J. Benkovic, D. Bensimon, and V. Croquette, *Real-time observation of bacteriophage T4 gp41 helicase reveals an unwinding mechanism*, Proc. Natl. Acad. Sci. USA **104** (2007), 19790–19795.

[37] M.D. Betterton, and F. Julicher, Phys. Rev. Lett. **91** (2003), 258103.

[38] M.D. Betterton, and F. Julicher, Phys. Rev. E Stat. Nonlin. Soft Matter Phys. **71** (2005), 011904.

[39] R.W. Richardson, and N.G. Nossal, *Characterization of the bacteriophage T4 gene 41 DNA helicase*, J. Biol. Chem. **264** (1989), 4725–4731.

[40] T.A. Cha, and B.M. Alberts, *Effects of the bacteriophage T4 gene 41 and gene 32 proteins on RNA primer synthesis: coupling of leading- and lagging-strand DNA synthesis at a replication fork*, Biochemistry **29** (1990), 1791–1798.

[41] J.B. Lee, R.K. Hite, S.M. Hamdan, X.S. Xie, C.C. Richardson, and A.M. van Oijen, Nature **439** (2006), 621–624.

[42] M.A. Trakselis, R.M. Roccasecca, J. Yang, A.M. Valentine, and S.J. Benkovic, J. Biol. Chem. **278** (2004), 49839–49849.

[43] M. Manosas, M.M. Spiering, Z. Zhuang, S.J. Benkovic, and V. Croquette, unpublished.

[44] A.M. Valentine, F.T. Ishmael, V.K. Shier, and S.J. Benkovic, Biochemistry **40** (2001), 15074–15085.

[45] S.W. Nelson, R. Kumar, and S.J. Benkovic, *RNA primer handoff in bacteriophage T4 DNA replication: The role of single-stranded DNA binding protein and polymerase accessory proteins*, J. Biol. Chem. **283** (2008), 22838–22846.

[46] T.A. Cha, and B.M. Alberts, J. Biol. Chem. **264** (1989), 12220–12225.

[47] A. Yildiz, J.N. Forkey, S.A. McKinney, T. Ha, Y.E. Goldman, and P.R. Selvin, *Myosin v walks hand-over-hand: single fluorophore imaging with 1.5 nm localization*, Science **300** (2003), 2061–2065.

[48] X. Zhuang, L.E. Bartley, H.P. Babcock, R. Russel, T. Ha, D. Herschlag, and S.Chu, Science **288**(2000), 2048–2051.

[49] S. Weiss, *Fluorescence spectroscopy of single biomolecules*, Science **283** (1999), 1676–1683.

[50] T. Funatsu, Y. Harada, M. Tokunaga, K. Saito, and T. Yanagida, *Imaging of single fluorescent molecules and individual ATP turnovers by single myosin molecules in aqueous solution*, Nature **374** (1995), 555–559.

[51] A. Ishijima, H. Kojima, T. Funatsu, M. Tokunaga, H. Higuchi, H. Tanaka, T. Yanagida, Cell **92** (1998), 161–171.